6/12/95

SANDIA REPORT

SAND94–0379 • UC–814
Unlimited Release
Printed June 1995

Yucca Mountain Site Characterization Project

Formulation and Numerical Analysis of Nonisothermal Multiphase Flow in Porous Media

M. J. Martinez

Prepared by
Sandia National Laboratories
Albuquerque, New Mexico 87185 and Livermore, California 94550
for the United States Department of Energy
under Contract DE-AC04-94AL85000

"Prepared by Yucca Mountain Site Characterization Project (YMSCP) participants as part of the Civilian Radioactive Waste Management Program (CRWM). The YMSCP is managed by the Yucca Mountain Project Office of the U.S. Department of Energy, DOE Field Office, Nevada (DOE/NV). YMSCP work is sponsored by the Office of Geologic Repositories (OGR) of the DOE Office of Civilian Radioactive Waste Management (OCRWM)."

Issued by Sandia National Laboratories, operated for the United States Department of Energy by Sandia Corporation.

Available to DOE and DOE contractors from
Office of Scientific and Technical Information
PO Box 62
Oak Ridge, TN 37831

Prices available from (615) 576-8401, FTS 626-8401

Available to the public from
National Technical Information Service
US Department of Commerce
5285 Port Royal Rd
Springfield, VA 22161

NTIS price codes
Printed copy: A03
Microfiche copy: A01

SAND94-0379
Unlimited Release
June 1995

Distribution
Category UC-814

Formulation and Numerical Analysis of Nonisothermal Multiphase Flow in Porous Media

M. J. Martinez
Engineering Sciences Center
Sandia National Laboratories
Albuquerque, NM 87185

Abstract

A mathematical formulation is presented for describing the transport of air, water and energy through porous media. The development follows a continuum mechanics approach. The theory assumes the existence of various average macroscopic variables which describe the state of the system. Balance equations for mass and energy are formulated in terms of these macroscopic variables. The system is supplemented with constitutive equations relating fluxes to the state variables, and with transport property specifications. Specification of various mixing rules and thermodynamic relations completes the system of equations. A numerical simulation scheme, employing the method of lines, is described for one-dimensional flow. The numerical method is demonstrated on sample problems involving nonisothermal flow of air and water. The implementation is verified by comparison with existing numerical solutions.

Acknowledgment

The author thanks R. H. Nilson for many helpful discussions. Reviews of the manuscript by R. R. Eaton and C. K. Ho are also greatly appreciated.

These Yucca Mountain Project activities are covered under WBS 1.2.5.4.1, Work Agreement WA0036.

This work was supported by the United States Department of Energy under contract DE-AC04-94AL85000.

This page intentionally left blank.

Table of Contents

List of Figures

This page intentionally left blank.

1. Introduction

There are several approaches leading to the development of a mathematical description of multiphase flow in porous media. This fact in itself is indicative of a state of flux in the development and understanding of multiphase flow in porous media. The basic problem lies in the fact that a pore scale description is impractical due to the complex geometries of the interstitial passages through which the fluids must flow. A more practical approach is to develop a description applicable to the macroscale, and herein lies the source of the problem. The equations governing multiphase flow on the microscale (Williams, 1985) are fairly well-established, although by no means fully settled. However, the problem of taking the microscale continuum equations to the macroscale is a formidable task. The approaches taken to date involve averaging methods, use of mixture theory, and a macroscale continuum approach (see Hassanizadeh and Gray, 1990). By the latter we refer to an approach where certain macroscale quantities are assumed to exist at the outset. In the present work, we will follow a continuum mechanics approach based on postulates regarding relations between microscale and macroscale quantities, although we make use of findings from all the aforementioned approaches. Balance equations for mass and energy are supplemented with constitutive equations, transport property specifications, and thermodynamic relations to complete the system of equations.

A numerical scheme, based on the so-called Method-of-Lines (MOL, Hyman, 1979) is described and implemented for one-dimensional flow. Here, the spatial derivatives are approximated by finite differences, resulting in a system of ordinary differential equations describing the temporal variation of variables as nodes. The system is integrated in time using existing variable-step variable-order solvers for systems of stiff differential equations.

This work is relevant to the development of mathematical and numerical models to treat multiphase flow in discretely fractured porous materials. A particular motivation for this work was to develop a numerical model for estimation of vapor-phase moisture transport from Yucca Mountain. This flow process may be of importance to the evaluation of Yucca Mountain as a potential site for a high-level radioactive waste repository. The present work represents the first step toward this goal, and involves flow in a single porous continuum. The model described here has been extended to treat discretely fractured media. An enhanced version of the present code was applied to estimate the net annual efflux of moisture from Yucca Mountain due to barometrically induced fluctuations in atmospheric pressure (Chapter 22 of Wilson, *et al.*, 1994). It is noted that several codes exist which were developed to model nonisothermal multiphase flow in porous media (Zyvoloski *et al.*, 1993; Pruess, 1987), however none appear adequate to model flow in discretely fractured media. Results of the study by Martinez and Nilson, in Chapter 22 of Wilson *et al.* indicate that the barometric pumping of moisture could only be modeled with a discrete fracture theory. The formulation in that work is of the multiple continuum type. Including the coupled equations describing fracture and matrix into either of the aforementioned codes appeared to be more involved than the approach ultimately chosen, which is discussed in Wilson, *et al.* (1994).

2. Balance Equations

2.1 Continuity Equations

The system under consideration is composed of a porous matrix or skeleton whose interstitial volume is occupied by fluid in motion under various forces. The interstitial volume or porosity is denoted ϕ and is occupied by both a liquid and gas phase. For definiteness, we take the fluid components to be air and water, where the former is supposed to exist only in the gaseous phase and the latter can exist as liquid and vapor; the gas phase is a mixture of air and water vapor. In the remainder of this work, subscript g refers to gas, v to water vapor, a to air, l to liquid, and m to moisture (e.g., liquid and vapor). Several balance equations can be written in terms of the various phases and components. We will develop each of these as they will be useful in the ensuing discussion, even though we ultimately base the model on certain combinations of these balance equations.

A balance equation for the liquid phase (liquid water) takes the form

$$\frac{\partial}{\partial t}(\rho_l \theta_l) + \nabla \bullet \boldsymbol{F}_l = -m_v \,, \tag{1}$$

where ρ_l is the liquid density, θ_l is the volumetric liquid content, $\boldsymbol{F}_l$ is the liquid mass flux vector, and m_v is the rate of evaporation of liquid. A balance equation for the gas phase, a mixture of air and water vapor, takes the form

$$\frac{\partial}{\partial t}(\rho_g \theta_g) + \nabla \bullet \boldsymbol{F}_g = m_v \,, \tag{2}$$

where ρ_g is the gas mixture density, θ_g is the volumetric gas content, and $\boldsymbol{F}_g$ is the gas mass flux vector. The liquid and gas fully occupy the porosity

$$\theta_l + \theta_g = \phi. \tag{3}$$

Since the gas phase is a mixture of air and water vapor, we may wish to consider balance equations for each of these components. A balance of water vapor is given by

$$\frac{\partial}{\partial t}(\rho_v \theta_g) + \nabla \bullet \boldsymbol{F}_v = m_v \,, \tag{4}$$

where ρ_v denotes the vapor density and $\boldsymbol{F}_v$ is the flux of water vapor, respectively. A balance of air reads

$$\frac{\partial}{\partial t}(\rho_a \theta_g) + \nabla \bullet \boldsymbol{F}_a = 0 \,, \tag{5}$$

where the subscript a refers to air.

Because the gas is a mixture (air is treated here as an identifiable component, even though it is also a compound), each component will undergo interdiffusion whenever a gradient in

concentration exists (see, for example, Bird, Stewart and Lightfoot, 1960). On average, the gas mixture as a whole moves with the average mass flux

$$F_g \equiv \rho_g q_g = F_v + F_a , \tag{6}$$

where q_g is the gas flux per unit area of porous medium. However, each component can also diffuse relative to this average mass flux, and so each can move with a different mass flux vector. Thus, the net flux of each gas component has a contribution due to diffusion in addition to the pressure-driven advective part. The latter contribution is presumed to be given in proportion to the local concentration of the considered component. For example, the net mass flux of water vapor relative to stationary coordinates, is given by

$$F_v = \rho_v q_g + J_v = X_v \rho_g q_g + J_v , \tag{7}$$

where J_v denotes the diffusion flux of water vapor in air, and the mass fraction of water vapor is introduced as

$$X_v = \frac{\rho_v}{\rho_g} . \tag{8}$$

Similarly, the net flux of air in the gas phase is given by

$$F_a = X_a \rho_g q_g + J_a . \tag{9}$$

Clearly, in order for the sum of air and water vapor mass fluxes to equal the mass flux of gas as defined in (6),

$$J_a + J_v = 0 , \tag{10}$$

where we have used the relation that $X_v + X_a = 1$.

The difficulty with utilizing the balance of liquid and gas in a mathematical model is the appearance of the rate of evaporation of individual components in a particular phase. A constitutive relation for the rate of evaporation/condensation is required if this form of the balance equations is to be the basis of a mathematical description. Equations of this form have been used by Hadley, 1985, and Bixler, 1985, but required the use of an *ad hoc* relation for the rate of evaporation of water. The method used by Bixler to obtain numerical solutions was to set the time constant in the rate expression to be smaller than any other physical timescale in the problem, thus forcing the water vapor to be nearly in thermodynamic equilibrium. The drawback of this scheme is that making the timescale for evaporation short forces the timescale for accurate and stable integrations to also be smaller than all other physical timescales. This artificially introduces additional stiffness into the system, since regions with large temperature gradients have much shorter local time-constants than regions with small temperature gradients. The overall numerical scheme may consequently suffer in performance.

An alternative multicomponent formulation involves forming a cumulative balance equation for each component which sums the mass of that component in all possible phases.

This eliminates the sources present in a balance equation for a single constituent in a particular phase. This form does, however, present other peculiarities related to the formulation of allowable boundary conditions and to sorting out the thermodynamic state of each component. In the present work, this alternative formulation amounts to forming a balance equation for matrix water, including liquid and vapor phases, given by summing (1) and (4),

$$\frac{\partial}{\partial t}(\rho_l\theta_l + \rho_v\theta_g) + \nabla\bullet\boldsymbol{F}_m = 0 \ , \tag{11}$$

where the net flux of moisture is

$$\boldsymbol{F}_m = \rho_l\boldsymbol{q}_l + X_v\rho_g\boldsymbol{q}_g + \boldsymbol{J}_v \ . \tag{12}$$

To reiterate, starting from the left, the terms on the RHS represent the mass flux of liquid, the advective mass flux of water vapor and the diffusive flux of water vapor, respectively. The balance of water (11) together with the balance of air (5) form the necessary continuity equations for the mathematical description.

2.2 Energy Balance

The multiphase system is assumed to be in thermal equilibrium. In particular, the thermal energy state of the fluids and solid in a representative elementary volume (REV) is described by a single average temperature, T. An energy balance takes the form

$$\frac{\partial}{\partial t}U + \nabla\bullet\boldsymbol{q}_h = Q \ , \tag{13}$$

where

$$U = (1-\phi)\rho_s u_s + \theta_l\rho_l u_l + \theta_g\rho_g u_g \tag{14}$$

is the bulk internal energy composed of the three phases, each defined with respect to the constant volume specific heats,

$$\begin{aligned} u_s &= C_s(T-T_0) \\ u_l &= C_l(T-T_0) \\ u_g &= C_g(T-T_0) \end{aligned} \tag{15}$$

and the heat capacity of the gas is

$$C_g = C_{va}X_a + C_{vv}X_v \ . \tag{16}$$

Also, $\boldsymbol{q}_h$ denotes the net heat flux vector, including diffusive and advective transport of heat, $C_{v\alpha}$ is the constant volume specific heat of component α, T_0 is a reference temperature, and Q is an extraneous heat source.

3. Constitutive Relations

In order to close the system of equations, one must now propose constitutive equations which provide relations between the kinematic variables appearing in the balance equations and the state variables.

3.1 Flux Relations

In describing flow through porous media, one must necessarily pose average quantities rather than pore-scale continuum values. For example, even though the Darcy fluxes, q, have units of velocity, they represent the local volume flux per unit area of porous medium. As such, they cannot satisfy the no-slip condition on boundaries. The flux relations to follow take the place of the momentum balance in continuum equations; they are the average momentum balances under conditions of "creeping flow," i.e., inertia-free, slow viscous flow.

The advective fluxes are assumed to be adequately described by the extended Darcy law, in which relative permeabilities are introduced to account for the multiphase motion of fluids. Thus the mass flux of liquid is

$$\rho_l q_l = F_l = -\frac{\rho_l k k_{rl}}{\mu_l}(\nabla P_l + \rho_l g \nabla z) \tag{17}$$

and the mass flux of gas is

$$\rho_g q_g = F_g = -\frac{\rho_g k k_{rg}}{\mu_g}(\nabla P_g + \rho_g g \nabla z) \ , \tag{18}$$

where P is pressure, g is the gravitational acceleration, and μ is dynamic viscosity. The intrinsic permeability of the medium is k and the relative permeabilities are denoted k_{rl} and k_{rg}, for liquid and gas, respectively.

The diffusive flux of water vapor in air is given by

$$J_v = -\rho_g D_{va} \nabla X_v \ . \tag{19}$$

We note here that this form is only valid for binary mixtures. In a multicomponent system with more than two components, the diffusion fluxes appear in the so-called Stefan-Maxwell form (see Appendix E of Williams, 1985) which is an implicit system of equations for the diffusive fluxes in terms of the gradients of mass fraction.

The total heat flux vector includes conduction and convective contributions,

$$q_h = -\lambda \nabla T + h_v F_v + h_a F_a + h_l F_l \tag{20}$$

where λ is an effective thermal conductivity (see Section 3.4). The enthalpies are defined by $h_\alpha = C_{p\alpha}(T - T_0)$, with $\alpha = a$ or l, and $h_v = \Delta h_{fg} + C_{pl}(T - T_0)$, where Δh_{fg} is the latent heat of water vapor at reference temperature T_0.

3.2 Mixture Relations and Thermodynamics

Ideal gas equations of state and mixing rules are used to approximate the thermodynamics of the system. Thus,

$$P_v = \rho_v R_v T \qquad P_a = \rho_a R_a T \tag{21}$$

with $R_\alpha = \Re / M_\alpha$, where $\Re$ is the gas constant, $\alpha = v$ or a, and M_α denotes the molecular weight. Also

$$\rho_g = \rho_v + \rho_a \qquad P_g = P_v + P_a \,. \tag{22}$$

The vapor pressure is specified according to Kelvin's equation of vapor pressure lowering (Edlefsen and Anderson, 1943),

$$P_v = P_{vs}(T)\, exp\left(-\frac{P_c}{\rho_l R_v T}\right), \tag{23}$$

where P_{vs} denotes the flat-interface saturation vapor pressure, and P_c is the capillary pressure. Note that this relation is derived via a microscale argument (Edlefsen and Anderson, 1943), whereas here we assume that the same relation holds on the macroscale, with all quantities defined as averages over the REV.

Over a wide range of temperatures, a function in the form of a Clapeyron equation adequately describes the flat-interface vapor density as a function of temperature,

$$\rho_{vs} = \rho_{v,ref} exp\left(\frac{\Delta h_{fg}}{R_v}\left(T_{ref}^{-1} - T^{-1}\right)\right) = A e^{-B/T}, \tag{24}$$

with $A = 7.055\text{x}10^5$ kg/m^3, and $B = 5137.46$ K[1], and the saturation pressure is determined from the ideal gas law, $P_{vs} = \rho_{vs} R_v T$. In this model, we will assume that water always exists in liquid and vapor phases, otherwise the vapor pressure is independent of temperature in the superheated regime.

3.3 Capillary Pressure

Because the transport problem under consideration involves liquid and vapor phases, it is reasonable to assume that capillary forces may be important. Kelvin's equation for vapor pressure lowering introduces the capillary pressure,

1. These parameters are temperature dependent and these values are accurate for $T < 70\ ^\circ$C.

$$P_c \equiv P_g - P_l = \hat{P}_c(\theta_l) \ , \tag{25}$$

which, as indicated, is assumed to be empirically specified as a function of liquid moisture content. Here again, the capillary pressure as defined is well motivated on the microscale. Its interpretation on the macroscale is not so easily motivated, and involves postulating the existence of the relation relative to REV-averaged pressures. The capillary pressure-moisture content relation is commonly assumed to hold for flow in porous media.

3.4 Transport Parameters

3.4.1 Moisture retention and relative permeability functions

A fundamental specification is the relation between volumetric liquid moisture content and capillary pressure, commonly referred to as the moisture retention curve. A popular and somewhat general form for the relation between capillary pressure and liquid moisture content is described by the so-called van Genuchten equation (van Genuchten, 1978),

$$\frac{\theta_l - \theta_{lr}}{\phi - \theta_{lr}} = \left(1 + p_c^{\beta_v}\right)^{-\lambda_v} \tag{26}$$

where θ_{lr} is the irreducible or residual moisture content, $p_c = \alpha_v P_c / \rho_l g$ and $\lambda_v = (\beta_v - 1)/\beta_v$. Both α_v and β_v are empirical material-dependent parameters that typically require laboratory measurement. The corresponding relative permeability to the liquid is given by (van Genuchten, 1978)

$$k_{rl} = \left(1 + p_c^{\beta_v}\right)^{-\lambda_v/2} \left[1 - \left(\frac{p_c^{\beta_v}}{1 + p_c^{\beta_v}}\right)^{\lambda_v}\right]^2 . \tag{27}$$

The relative permeability to the gas is approximated by the relation (Bixler, 1985, Pruess, 1987)

$$k_{rl} + k_{rg} = 1 \ . \tag{28}$$

We note that these specific functions are currently included in the numerical model; however, other forms are also easily incorporated.

3.4.2 Binary diffusion

The diffusion coefficient is pressure and temperature dependent (Vargaftik, 1975; Pruess, 1987),

$$D_{va} = \frac{\theta_g}{\tau} D_{va}^0 \frac{P_{ref}}{P_g} \left(\frac{T}{T_{ref}}\right)^v \ , \tag{29}$$

where τ is tortuosity and D_{va}^{0} is the diffusivity in free space at temperature T_{ref} and pressure P_{ref}. The term θ_g/τ modifies the expression for free diffusion to account for the porous skeleton.

3.4.3 Effective conductivity

The liquid-saturation-dependent effective heat conductivity is specified according to (Somerton, *et al.*, 1974),

$$\lambda = \lambda_0 + \frac{\theta_l}{\phi}(\lambda_1 - \lambda_0) \; . \tag{30}$$

Given this functional relation with respect to moisture content, λ_0 is the conductivity under dry conditions, and λ_1 is the conductivity under fully saturated conditions. The numerical model to be described next, is programmed with the foregoing transport functions. Other, different specific functions can also be specified by the user.

This completes the specification of auxiliary data required to complete the mathematical model of nonisothermal multiphase flow through a porous medium. The resulting model is seen to be highly nonlinear and numerical methods are generally required for obtaining approximate solutions to boundary value problems.

4. Numerical Treatment

The flow equations describing the transport of water, air and energy are comprised of the water balance (11), the air balance, (5) and the energy balance (13), together with equations of constitution and transport parameters. In this work, we treat only two-phase flow, i.e., water vapor and liquid water are always present. Thus, the set of state or primary variables are chosen to be the capillary pressure, the gas pressure, and temperature. The capillary pressure is associated with the water balance equation, the gas pressure with the air balance and temperature with the energy equation, see Eqn. 31 below.

The governing equations constitute a coupled set of highly nonlinear partial differential equations (PDEs). The numerical method applied for solving the coupled system of parabolic PDEs is the so-called Method-of-Lines (MOL) (Hyman, 1979). The MOL technique is a semidiscretization method wherein the spatial derivatives are first approximated by some appropriate method (in this case, finite differences), resulting in a system of coupled ordinary differential equations (ODEs) describing the temporal variation of the state variables at a number of discrete points or nodes. The effective treatment of the highly nonlinear system considered here is made possible by the availability of highly optimized ODE solvers (Shampine and Watts, 1980). In the present work, the spatial derivatives are approximated by a centered difference approximation. The resulting system of ODEs is integrated forward in time by the variable-order, variable-step backward-difference code DEBDF (Shampine and Watts, 1980). The backward-difference formulae result in systems of nonlinear algebraic equations to be solved for nodal quantities. These equations are solved as part of the DEBDF package via a Newton-type algorithm.

4.1 Canonical Form

In this model, we treat only one-dimensional transport. Approximating the spatial divergences by central differences, the system of discrete ODEs describing the temporal variation of primary variables at node points takes the form

$$\begin{bmatrix} C_\psi & 0 & C_{\psi T} \\ C_{p\psi} & C_P & C_{PT} \\ C_{T\psi} & C_{TP} & C_T \end{bmatrix}_i \begin{bmatrix} \dot{P}_c \\ \dot{P}_g \\ \dot{T} \end{bmatrix}_i = \frac{1}{x_{i+1/2} - x_{i-1/2}} \begin{bmatrix} F_{m,i+1/2} - F_{m,i-1/2} \\ F_{a,i+1/2} - F_{a,i-1/2} \\ q_{h,i+1/2} - q_{h,i-1/2} \end{bmatrix} + \begin{bmatrix} 0 \\ 0 \\ Q \end{bmatrix}_i \tag{31}$$

for a mesh of nodes with node points at x_i. At each mesh point the 3x3 matrix can be solved for the time derivatives of each state variable. The net moisture flux appearing in this equation is defined by $F_m = F_l + F_v$. Each flux is also expressed as a central difference (on a staggered mesh), for example

$$F_{l,i+1/2} = -\left(\frac{\rho_l k k_{rl}}{\mu_l} \right)_{i+1/2} \frac{P_{l,i+1} - P_{l,i}}{x_{i+1} - x_i}, \tag{32}$$

where $P_l = P_g - P_c$ is the liquid pressure. The definition of each entry in the capacitance matrix can be determined by considering the differential equation from which it was derived. The capacitance matrix is defined as,

$$\begin{bmatrix} C_\psi & 0 & C_{\psi T} \\ C_{p\psi} & C_P & C_{PT} \\ C_{T\psi} & C_{TP} & C_T \end{bmatrix}^T = \begin{bmatrix} \frac{\partial}{\partial P_c} \\ \frac{\partial}{\partial P_g} \\ \frac{\partial}{\partial T} \end{bmatrix} \begin{bmatrix} (\rho_l \theta_l + \rho_v \theta_g) & (\rho_a \theta_g) & U \end{bmatrix}. \tag{33}$$

The Appendix records more detailed entries in the matrix.

4.2 Boundary Conditions

Both Dirichlet and specified flux boundary conditions can be imposed on the discrete equations. Several combinations of Dirichlet and flux conditions are also allowable. The several types are discussed in the following. For a mesh of length L, the nodes are numbered 1 to N, and boundary fluxes are denoted with subscripts 1 and N.

4.2.1 Dirichlet conditions

The time variations at boundary nodes of all three degrees-of-freedom (DOF) are simply specified directly into the system of ODEs. For node 1,

$$\begin{bmatrix} \dot{P}_{c,1} \\ \dot{P}_{g,1} \\ \dot{T}_1 \end{bmatrix} = \frac{\partial}{\partial t} \begin{bmatrix} P_c(t) \\ P_g(t) \\ T(t) \end{bmatrix}_{x=0} , \tag{34}$$

with a similar equation for the Nth node, if Dirichlet conditions are specified at $x=L$.

4.2.2 Flux conditions

By performing a material or energy balance on the half-cell adjacent to the boundary, fluxes of the conserved quantities can be imposed,

$$\begin{bmatrix} C_\psi & 0 & C_{\psi T} \\ C_{p\psi} & C_P & C_{PT} \\ C_{T\psi} & C_{TP} & C_T \end{bmatrix}_1 \begin{bmatrix} \dot{P}_c \\ \dot{P}_g \\ \dot{T} \end{bmatrix}_1 = \frac{2}{x_2 - x_1} \begin{bmatrix} F_{m,1} - F_{m,3/2} \\ F_{a,1} - F_{a,3/2} \\ q_{h,1} - q_{h,3/2} \end{bmatrix} + 2 \begin{bmatrix} 0 \\ 0 \\ Q \end{bmatrix}_1 . \tag{35}$$

where the 1-subscripted fluxes are specified (or set to zero for no-flux conditions). Note that these fluxes can be general functions of time. A similar equation applies at the Nth node if the fluxes are specified at $x=L$.

Note that in specifying any of these fluxes, there are several physical fluxes which are superposed in these definitions. For example, one may want to specify the injection of cold water at a mass flux rate F_{in}, at temperature T_{cold} together with an additional heat flux imposed at the same boundary. The mass flow rate of water is specified as $F_{m,1} = F_{in}$. The net heat flux is specified by superposing the enthalpy of the injected fluid with the conducted heat flux, q_{cond}, by specifying $q_{h,1} = q_{cond} + C_{pl}(T_{cold} - T_0) F_{in}$.

4.2.3 Mixed conditions

In many applications one may want to specify mixed boundary conditions, i.e., certain combinations of fluxes and primary variables. One may want to specify a temperature and impervious flow conditions on the fluids, for example. Assuming the conditions are specified at $x=0$, the specified temperature function is imposed as $\dot{T}_1 = dT(x=0)/dt$ in (31). This identity replaces the last equation in the matrix. Setting values of $F_{m,1}$, and $F_{a,1}$, (equal zero for impervious conditions) and moving the terms involving dT_1/dt to the RHS produces a 2x2 matrix to be solved for the time derivatives of capillary and gas pressure,

$$\begin{bmatrix} C_\psi & 0 \\ C_{p\psi} & C_P \end{bmatrix}_1 \begin{bmatrix} \dot{P}_c \\ \dot{P}_g \end{bmatrix}_1 = - \begin{bmatrix} C_{\psi T}\dot{T} \\ C_{PT}\dot{T} \end{bmatrix}_1 - \frac{2}{x_2 - x_1} \begin{bmatrix} F_m \\ F_a \end{bmatrix}_1 \tag{36}$$

This procedure generalizes for any combination with one Dirichlet DOF and two flux DOFs.

When two Dirichlet DOF are specified, these are substituted directly into the matrix (31), thereby replacing those equations with the identities specifying the time derivatives. The equation involving the flux DOF can then be solved for the time derivative of its corresponding state variable. For example, if the capillary pressure (or liquid saturation) and temperature are specified, then the ODE for the gas pressure is

$$C_P \dot{P}_g = -C_{\psi T}\dot{T} - C_{PT}\dot{P}_c - \frac{2}{x_2 - x_1} F_a \,, \tag{37}$$

where all quantities refer to node 1 (x=0), in this case. A similar equation applies if the boundary conditions are applied at x=L.

5. Test Problems

Several two-phase flow problems were simulated with the present MOL code in order to verify the numerical implementation. The first example problem involves the injection of heat into a one-dimensional horizontal column of porous material 2 m in length (L). The void volume is filled with air and water (liquid and vapor). The end (x=L) of the column opposite the heat injection is maintained at initial conditions, T=70° C, P_g=1 atm (.10133 MPa), and $S_l = \theta_l/\phi = 0.5$. A heat flux of 20 W/m^2 is applied at x=0; this boundary is also closed to flow of air and water. This value of heat flux is low enough that heat transport is mostly by conduction. The 2 m column was discretized into 100 evenly spaced cells.

The material properties specified for this problem are the same as in the steady heat pipe problems posed by Udell and Fitch (1985), to be discussed in the following. The capillary pressure-saturation relation is given by

$$P_c = \sigma\sqrt{\frac{\phi}{k}}\left(1.417\,(1-s) - 2.12\,(1-s)^2 + 1.263\,(1-s)^3\right) \tag{38}$$

and the relative permeabilities are defined by

$$k_{rg} = (1-s)^3 \qquad k_{rl} = s^3 \,, \tag{39}$$

where σ(=0.05878 N/m^2) denotes surface tension and

$$s = \frac{\theta_l - \theta_{lr}}{\phi - \theta_{lr}} \,. \tag{40}$$

The material has 40% porosity (ϕ) and 1 Darcy permeability (k=10^{-12} m^2). In addition, the effective thermal conductivity was specified as

$$\lambda = \lambda_0 + \sqrt{\frac{\theta_l}{\phi}}\,(\lambda_1 - \lambda_0) \tag{41}$$

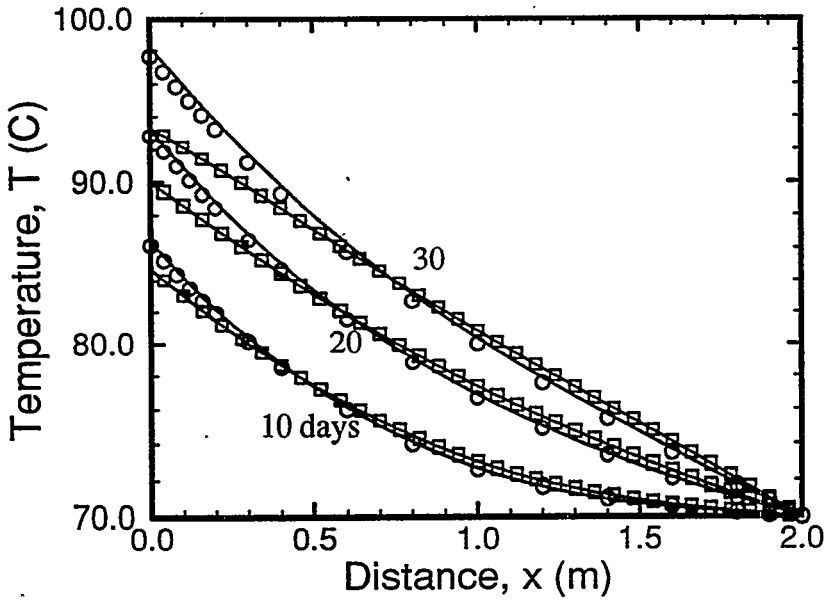

Figure 1 Temperature profiles due to a 20 W/m^2 heat flux given by the MOL (solid lines, no binary diffusion; solid lines with square symbols, diffusion included), and FEHMN (circles).

with λ_0=0.582 W/m-K and λ_1=1.13 W/m-K.

Figure 1 shows the evolution of temperature in the column over a 30 day simulation period. Also shown are the results of the simulation of the problem using the finite element multiphase code FEHMN developed by Zyvoloski *et al.*, (1993). A two-dimensional 100-element mesh was specified for discretizing the computation region (1x2 m), resulting in 202 node points at which the solution is calculated. The multiphase formulation in FEHMN does not include binary diffusion in the gas phase, and so the simulation with the MOL code was performed with and without diffusion, as indicated in the figure. When diffusion was included, the binary diffusion model outlined in Section 3 was applied with $\tau = 2$. The solutions without diffusion using FEHMN and the MOL compare well. The figure also illustrates the non-negligible influence of binary diffusion in the gas phase for a problem driven by even a moderate heat flux. The hotter temperatures increase the vapor pressure and so provide a concentration gradient which drives diffusion of water vapor to the cold end of the column. There is a corresponding decrease of liquid water content (i.e., drying) near the heat source (not shown).

The second test problem is similar to the one just described, except that it involves a higher rate of heat injection. This problem involves computing the steady heat pipe problem discussed by Udell and Fitch (1985). For purposes of comparison, the transient evolution to the steady solution was simulated and results compared with FEHMN. This problem exercises features of evaporation/condensation and vapor and liquid flows in the code. The material properties are the same as described in the preceding example. Once again, a 2 m horizontal column filled with water and air is considered, and the same discretizations as

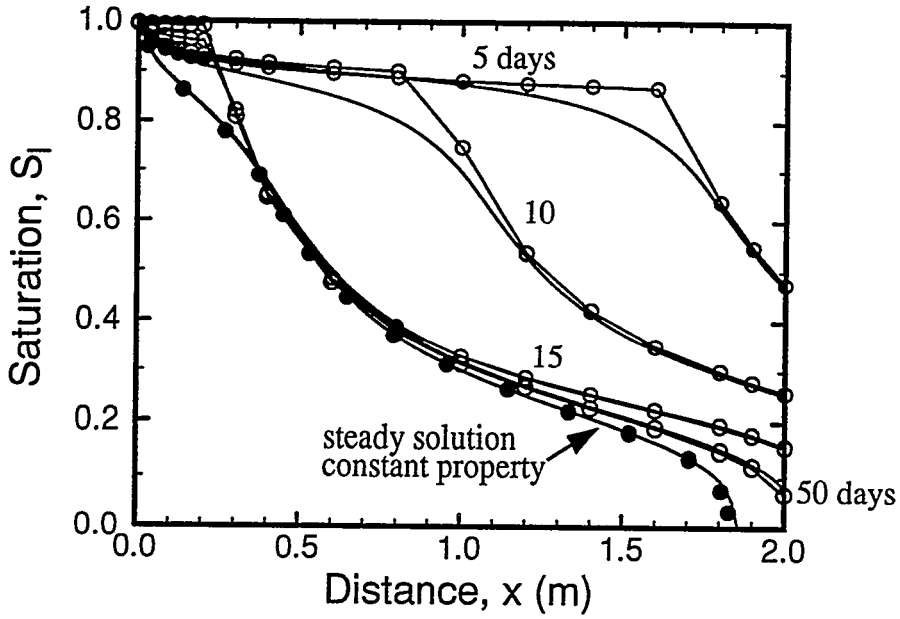

Figure 2 Comparison of saturation profiles given by the MOL (solid lines) and FEHMN (solid lines with open circles). The solid circles are the steady solution of Udell and Fitch (1985).

discussed above were used. Also, the same initial conditions were specified (T=70° C, P_g=1 atm, and S_l=0.5), but the boundary conditions differ. To initiate the transport, the left end (x=0) is abruptly saturated with liquid ($s_l = \theta_l/\phi = 1$), while the temperature and pressure are maintained at 70 °C and 0.10133 MPa, respectively. A 100 W/m^2 heat flux is applied at x=L, which is also closed to flow of air and water. This heat flux is of sufficient intensity to dry out the material in the steady solution of Udell and Fitch (1985).

Figures 2 and 3 show the transient evolution of liquid saturation and temperature as given by the MOL and FEHMN codes for up to 50 days of simulation, by which time a steady solution is attained. The MOL simulation includes binary diffusion of water vapor in air, and likely accounts for the discrepancy with the solution given by FEHMN, which neglects this mechanism. Figures 2 and 3 show the FEHMN solution to develop a kink in the solution profiles, due to the neglect of diffusion. (A simulation with the MOL for a very small diffusion coefficient displayed a similar result.) The corresponding steady solution given by FEHMN (50 days) displays a liquid-saturated region adjacent to the saturated boundary. Otherwise, the comparison between numerical solutions for saturation is good in the region between the kink and the heat source.

There are two different steady state MOL solutions shown in Figures 2 and 3. The steady solution, designated "constant property," was obtained by specifying constant kinematic viscosities in the Darcy relations for flux. The remaining solution curves shown in Figures 2 and 3 for the MOL were computed with variable, temperature-dependent properties as set forth in Section 3. The constant kinematic viscosity specification was made by Udell and Fitch, and was a necessary modification to the MOL code to obtain the steady state "constant property" solution shown. The consequence of this approximation is that the

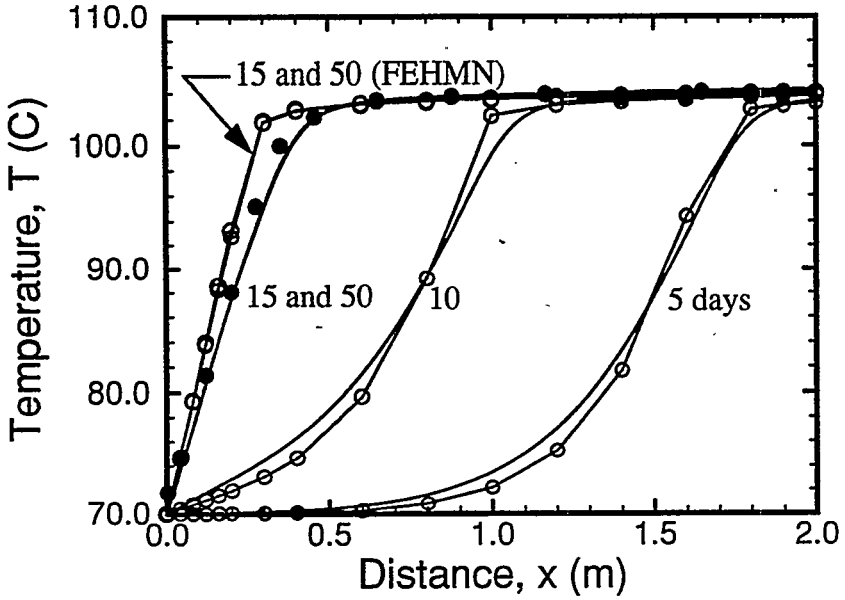

Figure 3 Comparison of temperature profiles given by the MOL (solid lines) and FEHMN (solid lines with open circles). The solid circles are the steady solution of Udell and Fitch (1985).

dynamic viscosities are assumed constant, but perhaps more important is that the gas density is also assumed constant. In contrast, the variable-property MOL simulation indicates about a 30% variation in gas density across the 2 m length, showing that assuming constant kinematic viscosity is not a good approximation in this case. Nevertheless, by specifying constant kinematic viscosity, the constant property steady solution obtained with the MOL compares very well with that of Udell and Fitch, including the mole fraction of air as shown in Figure 4. It is noted that, for a two-meter column, neither the FEHMN nor the MOL (variable property) steady solutions (50 days) indicate dry-out of the porous material, as is predicted by Udell and Fitch, and the constant property MOL solutions. Thus, the constant property specification reduces the length of the dry-out zone under present conditions.

Two other test problems computed with the two-phase, two-component MOL code can be mentioned here. As noted in the introduction, one motivation for the development of the present code was to model barometrically induced flows in fractured systems. A modified version of the code was developed to enable explicit modeling of fractures and matrix and is discussed in Chapter 22 of Wilson *et al.* (1994). Two benchmark problems are presented, including one which tests the method of coupling the fracture and matrix used in the barometric pumping problem. This test problem considers diffusive transport in a fracture/matrix system driven by an oscillating potential. Results for the net transport of conserved quantity compared very well with an analytic solution given by Nilson *et al.* (1991).

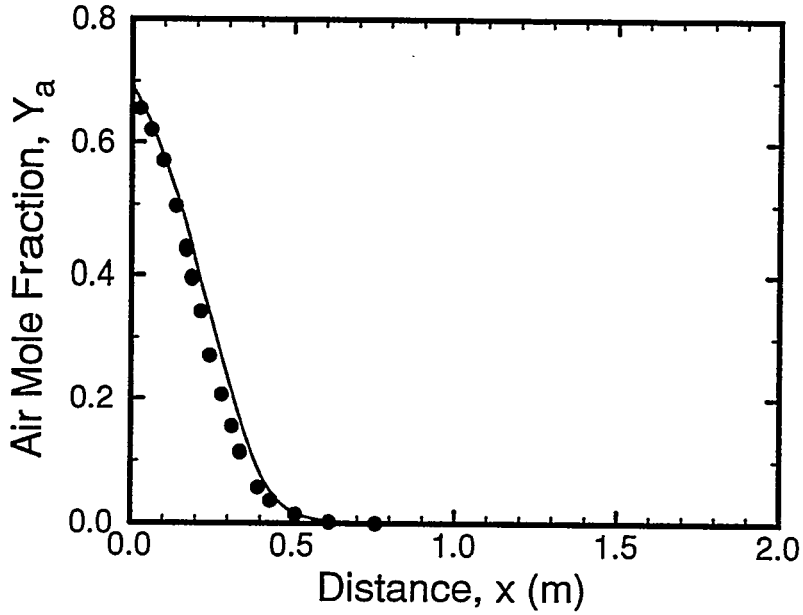

Figure 4 Comparison of the steady profiles of air mole fraction given by the MOL (solid line) and Udell and Fitch (1985) (solid circles).

6. Conclusions

We have presented a formulation describing nonisothermal multiphase transport of air, water and energy through porous media. The resulting system of highly nonlinear equations is simulated numerically by a method-of-lines procedure using finite-difference approximations for spatial gradients. The resulting code was applied to two nonisothermal two-phase flow problems. The implementation was partially verified by comparing the MOL solutions with existing numerical solutions.

The solutions generated with the MOL compared well with the steady solutions of Udell and Fitch (1985) which model a porous heat pipe problem. The MOL solutions also compared well with solutions generated with the finite element code FEHMN (Zyvoloski, *et al.*, 1993). This version of the code FEHMN (version fehm.7.0J) does not include binary diffusion in the gas phase. The MOL solutions, generated without and with diffusion, compared well with FEHMN for the former case, and illustrated the influence of binary diffusion in the latter case.

This page intentionally left blank.

7. References

Bird, R. B., W. E. Stewart, and E. N. Lightfoot, 1960, *Transport Phenomena*, Wiley, New York. NY. (NNA.900919.0195)

Bixler, N. E., 1985, NORIA - A finite element computer program for analyzing water, vapor, air, and energy transport in porous media, *SAND84-2057*, Sandia National Laboratories, Albuquerque, NM 115 pp. (NNA.870721.0002)

Edlefsen, N. E., and B. C. Anderson, 1943, Thermodynamics of soil moisture, *Hilgardia*, **15**(2), pp. 31-298. (NNA.900312.0151)

Hadley, G. R., 1985, PETROS -- A program for calculating transport of heat, water, water vapor, and air through a porous material, *SAND84-0878*, Sandia National Laboratories, Albuquerque, NM 67 pp. (NN1.881007.0038)

Hassanizadeh, M. S., and W. G. Gray, 1990, Mechanics and thermodynamics of multiphase flow in porous media including interphase boundaries, *Adv. Water Resources*, **13**(4), pp., 169-186. (NNA.940414.0113)

Hyman, J. M., 1979, A method of lines approach to the numerical solution of conservation laws, in *Advances in Computer Methods for Partial Differential Equations III*, R. Vichnevetsky and R. S. Stepleman, Eds., IMACS publications. (NNA.910405.0040)

Nilson, R. H., E. W. Peterson, K. H. Lie, N. R. Burkhard, and J. R Hearst, 1991, Atmospheric pumping: A mechanism causing vertical transport of contaminated gases through fractured permeable media, *J. Geophys. Res.*, **96** (B13), pp. 21933-21948. (NNA.940301.0029)

Pruess, K., 1987, TOUGH user's guide, *LBL-20700 (NUREG/CR-4645)*, Lawrence Berkeley Laboratory, Berkeley, CA 78 pp. (NNA.890315.0010)

Shampine, L. F., and H. A. Watts, 1980, DEPAC - Design of a user oriented package of ODE solvers, *SAND79-2374*, Sandia National Laboratories, Albuquerque, NM. (NNA.900122.0001)

Somerton, W. H., J. A. Keese, and S. L. Chu, 1974, Thermal behavior of unconsolidated oil sands, *SPE J.*, **14**(5), October. (NNA.890522.0271)

Udell, K. S., and J. S. Fitch, 1985, Heat and mass transfer in capillary porous media considering evaporation, condensation and non-condensable gas effects, presented at the 23rd ASME/AICHE National Heat Transfer Conference, Denver CO. (NNA.890713.0199)

van Genuchten, T., 1978, Calculating the unsaturated hydraulic conductivity with a new closed-form analytical model, *Water Resources Bulletin*, Princeton University Press, Princeton University, Princeton, NJ. (HQS.880517.1859)

Vargaftik, N. B., 1975, *Tables of the Thermophysical Properties of Liquids and Gases*, 2nd Ed., John Wiley and Sons, New York. (NNA.940428.0016)

Williams, F. A., 1985, *Combustion Theory*, 2nd Ed., Benjamin/Cummings Publ. Co. Inc., Menlo Park, CA. (NNA.940321.0122)

Wilson, M. L., Gauthier, J., R. W. Barnard, G. E. Barr, H. A. Dockery, E. Dunn, R. R. Eaton, D. C. Guerin, N. Lu, M. J. Martinez, R. H. Nilson, C. A. Rautman, T. H. Robey, B. Ross, E. E. Ryder, A. R. Schenker, S. A. Shannon, L. H. Skinner, W. G. Halsey, J. Gansemer, L. C., Lewis, A. D. Lamont, I. R. Triay, A. Meijer, and D. E. Morris, 1994, Total-system performance assessment for Yucca Mountain - SNL second iteration (TSPA-1993), *SAND93-2675*, Sandia National Laboratories, Albuquerque, NM. (NNA.940112.0123)

Zyvoloski, G., Z. Dash, and S. Kelkar, 1993, FEHMN 1.0: Finite element heat and mass transfer code, *LA-12062-MS, Rev. 1*, Los Alamos National Laboratory, Los Alamos, NM, 130 pp. (NNA.930921.0008)

APPENDIX

Details of the Capacitance Matrix

We record here the explicit definitions of the entries in the capacitance matrix **C**.

$$C_{\psi} = (\rho_l - \rho_v)\frac{\partial \theta_l}{\partial P_c} + \theta_g \frac{\partial \rho_v}{\partial P_c} \tag{42}$$

$$C_{\psi T} = (\rho_l - \rho_v)\frac{\partial \theta_l}{\partial T} + \theta_g \frac{\partial \rho_v}{\partial T} \tag{43}$$

$$C_{P\psi} = \theta_g \frac{\partial \rho_a}{\partial P_v}\frac{\partial P_v}{\partial P_c} - \rho_a \frac{\partial \theta_l}{\partial P_c} \tag{44}$$

$$C_P = \frac{\theta_g}{R_a T} \tag{45}$$

$$C_{PT} = \theta_g \left(\frac{\partial \rho_a}{\partial P_v}\frac{\partial P_v}{\partial T} - \frac{\rho_a}{T} \right) \tag{46}$$

$$C_{T\psi} = \rho_g \theta_g (C_{vv} - C_{va})(T - T_0)\frac{\partial X_v}{\partial P_c} + (\rho_l u_l - \rho_g u_g)\frac{\partial \theta_l}{\partial P_c} + u_g \theta_g \frac{\partial \rho_g}{\partial P_c} \tag{47}$$

$$C_{TP} = (\rho_g \theta_g)(C_{vv} - C_{va})(T - T_0)\frac{\partial X_v}{\partial P_g} + u_g \theta_g \frac{\partial \rho_g}{\partial P_g} \tag{48}$$

$$C_T = U + \rho_g \theta_g (C_{vv} - C_{va})(T - T_0)\frac{\partial X_v}{\partial T} + u_g \theta_g \frac{\partial \rho_g}{\partial T} \tag{49}$$

The internal energies are defined by

$$u_g = u_a + u_v = (X_a C_{va} + X_v C_{vv})(T - T_0)\,, \tag{50}$$

$$u_l = C_l (T - T_0)\,. \tag{51}$$

The remaining derivatives in the foregoing are obtained by operating on the appropriate relations defined in the body of the report, resulting in:

$$\frac{\partial \rho_v}{\partial P_c} = -\frac{\rho_v}{\rho_l R_v T}, \qquad \frac{\partial \rho_v}{\partial T} = -\frac{\rho_v}{T}\left(1 - \frac{P_c}{\rho_l R_v T}\right) + \frac{\rho_v}{P_{vs}}\frac{\partial P_{vs}}{\partial T} \tag{52}$$

$$\frac{\partial P_v}{\partial P_c} = -\frac{P_v}{\rho_l R_v T}, \qquad \frac{\partial P_v}{\partial T} = P_v\left(\frac{1}{P_{vs}}\frac{\partial P_{vs}}{\partial T} + \frac{P_c}{\rho_l R_v T^2}\right) \tag{53}$$

$$\frac{\partial \rho_g}{\partial P_g} = -\frac{\partial \rho_a}{\partial P_v} = \frac{\rho_a}{P_a} \tag{54}$$

$$\frac{\partial \rho_g}{\partial P_c} = \left(\frac{\rho_a}{P_a} - \frac{\rho_v}{P_v}\right)\frac{P_v}{\rho_l R_v T}, \qquad \frac{\partial \rho_g}{\partial T} = -\frac{\rho_g}{T} - \left(\frac{\rho_a}{P_a} - \frac{\rho_v}{P_v}\right)\frac{\partial P_v}{\partial T} \tag{55}$$

$$\frac{\partial X_v}{\partial P_c} = -\frac{X_v}{\rho_l R_v T}\left[1 - X_v\left(1 - \frac{M_a}{M_v}\right)\right], \qquad \frac{\partial X_v}{\partial P_g} = -\frac{X_v^2 M_a}{P_v M_v}. \tag{56}$$

$$\frac{\partial X_v}{\partial T} = X_v\left[1 - X_v\left(1 - \frac{M_a}{M_v}\right)\right]\left[\frac{1}{P_{vs}}\frac{\partial P_{vs}}{\partial T} + \frac{P_c}{\rho_l R_v T^2}\right]. \tag{57}$$

YUCCA MOUNTAIN SITE CHARACTERIZATION PROJECT

UC814 - DISTRIBUTION LIST

1 D. A. Dreyfus (RW-1)
Director
OCRWM
US Department of Energy
1000 Independence Avenue SW
Washington, DC 20585

1 L. H. Barrett (RW-2)
Acting Deputy Director
OCRWM
US Department of Energy
1000 Independence Avenue SW
Washington, DC 20585

1 J. D. Saltzman (RW-4)
Office of Strategic Planning and
International Programs
OCRWM
US Department of Energy
1000 Independence Avenue SW
Washington, DC 20585

1 J. D. Saltzman (RW-5)
Office of External Relations
OCRWM
US Department of Energy
1000 Independence Avenue SW
Washington, DC 20585

1 Samuel Rousso (RW-10)
Office of Program and Resource Mgt.
OCRWM
US Department of Energy
1000 Independence Avenue SW
Washington, DC 20585

1 J. C. Bresee (RW-10)
OCRWM
US Department of Energy
1000 Independence Avenue SW
Washington, DC 20585

1 S. Rousso (RW-50)
Office of Contract Business
Management
OCRWM
US Department of Energy
1000 Independence Avenue SW
Washington, DC 20585

1 R. M. Nelson (RW-20)
Office of Geologic Disposal
OCRWM
US Department of Energy
1000 Independence Avenue SW
Washington, DC 20585

1 S. J. Brocoum (RW-22)
Analysis and Verification Division
OCRWM
US Department of Energy
1000 Independence Avenue SW
Washington, DC 20585

1 D. Shelor (RW-30)
Office of Systems and Compliance
OCRWM
US Department of Energy
1000 Independence Avenue SW
Washington, DC 20585

1 J. Roberts (RW-33)
Director, Regulatory Compliance
Division
OCRWM
US Department of Energy
1000 Independence Avenue SW
Washington, DC 20585

1 G. J. Parker (RW-332)
Reg. Policy/Requirements Branch
OCRWM
US Department of Energy
1000 Independence Avenue SW
Washington, DC 20585

1 R. A. Miller (RW-40)
Office of Storage and
Transportation
OCRWM
US Department of Energy
1000 Independence Avenue SW
Washington, DC 20585

1 D. R. Elle, Director
Environmental Protection and Division
DOE Nevada Field Office
US Department of Energy
P.O. Box 98518
Las Vegas, NV 89193-8518

1 T. Wood (RW-52)
Director, M&O Management Division
OCRWM
US Department of Energy
1000 Independence Avenue SW
Washington, DC 20585

4 Victoria F. Reich, Librarian
Nuclear Waste Technical Review Board
1100 Wilson Blvd., Suite 910
Arlington, VA 22209

5 Wesley Barnes, Project Manager
Yucca Mountain Site
Characterization Office
US Department of Energy
P.O. Box 98608--MS 523
Las Vegas, NV 89193-8608

1 C. L. West, Director
Office of External Affairs
DOE Nevada Field Office
US Department of Energy
P.O. Box 98518
Las Vegas, NV 89193-8518

8 Technical Information Officer
DOE Nevada Field Office
US Department of Energy
P.O. Box 98518
Las Vegas, NV 89193-8518

1 P. K. Fitzsimmons, Technical Advisor
Office of Assistant Manager for
Environmental Safety and Health
DOE Nevada Field Office
US Department of Energy
P.O. Box 98518
Las Vegas, NV 89193-8518

1 J. A. Blink
Deputy Project Leader
Lawrence Livermore National Lab.
101 Convention Center Drive
Suite 820, MS 527
Las Vegas, NV 89109

4 J. A. Canepa
Technical Project Officer - YMP
N-5, Mail Stop J521
Los Alamos National Laboratory
P.O. Box 1663
Los Alamos, NM 87545

1 H. N. Kalia
Exploratory Shaft Test Manager
Los Alamos National Laboratory
Mail Stop 527
101 Convention Center Dr., #820
Las Vegas, NV 89101

1 Repository Licensing & Quality Assurance
Project Directorate
Division of Waste Management
US NRC
Washington, DC 20555

1 Senior Project Manager for Yucca Mountain
Repository Project Branch
Division of Waste Management
US NRC
Washington, DC 20555

1 NRC Document Control Desk
Division of Waste Management
US NRC
Washington, DC 20555

1 Chad Glenn
NRC Site Representative
301 E Stewart Avenue, Room 203
Las Vegas, NV 89101

1 E. P. Binnall
Field Systems Group Leader
Building 50B/4235
Lawrence Berkeley Laboratory
Berkeley, CA 94720

1 Center for Nuclear Waste Regulatory Analyses
6220 Culebra Road
Drawer 28510
San Antonio, TX 78284

3 W. L. Clarke
Technical Project Officer - YMP
Attn: YMP/LRC
Lawrence Livermore National Laboratory
P.O. Box 5514
Livermore, CA 94551

1 V. R. Schneider
Asst. Chief Hydrologist--MS 414
Office of Program Coordination and Technical Support
US Geological Survey
12201 Sunrise Valley Drive
Reston, VA 22092

1 J. S. Stuckless
Geologic Division Coordinator
MS 913
Yucca Mountain Project
US Geological Survey
P.O. Box 25046
Denver, CO 80225

1 N. Z. Elkins
Deputy Technical Project Officer
Los Alamos National Laboratory
Mail Stop 527
101 Convention Center Drive, #820
Las Vegas, NV 89101

5 L. S. Costin, Acting
Technical Project Officer - YMP
Sandia National Laboratories
Organization 6302, MS 1333
P.O. Box 5800
Albuquerque, NM 87185

1 J. F. Devine
Asst Director of Engineering Geology
US Geological Survey
106 National Center
12201 Sunrise Valley Drive
Reston, VA 22092

1 L. R. Hayes
Technical Project Officer
Yucca Mountain Project Branch
MS 425
US Geological Survey
P.O. Box 25046
Denver, CO 80225

1 A. L. Flint
US Geological Survey
MS 721
P.O. Box 327
Mercury, NV 89023

1 D. A Beck
Water Resources Division, USGS
6770 S. Paradise Road
Las Vegas, NV 89119

1 P. A. Glancy
US Geological Survey
Federal Building, Room 224
Carson City, NV 89701

1 Sherman S. C. Wu
US Geological Survey
2255 N. Gemini Drive
Flagstaff, AZ 86001

1 J. H. Sass - USGS
Branch of Tectonophysics
2255 N. Gemini Drive
Flagstaff, AZ 86001

1 D. H. Appel, Chief
Hydrologic Investigations Program
MS 421
US Geological Survey
P.O. Box 25046
Denver, CO 80225

1 E. J. Helley
Branch of Western Regional Geology
MS 427
US Geological Survey
345 Middlefield Road
Menlo Park, CA 94025

1 R. W. Craig, Chief
Nevada Operations Office
US Geological Survey
101 Convention Center Drive
Suite 860, MS 509
Las Vegas, NV 89109

1 D. Zesiger
US Geological Survey
101 Convention Center Drive
Suite 860, MS 509
Las Vegas, NV 89109

1 G. L. Ducret, Associate Chief
Yucca Mountain Project Division
US Geological Survey
P.O. Box 25046
421 Federal Center
Denver, CO 80225

2 L. D. Foust
Nevada Site Manager
TRW Environmental Safety Systems
101 Convention Center Drive
Suite 540, MS 423
Las Vegas, NV 89109

1 C. E. Ezra
YMP Support Office Manager
EG&G Energy Measurements Inc.
MS V-02
P.O. Box 1912
Las Vegas, NV 89125

1 Jan Docka
Roy F. Weston, Inc.
955 L'Enfant Plaza SW
Washington, DC 20024

1 Technical Information Center
Roy F. Weston, Inc.
955 L'Enfant Plaza SW
Washington, DC 20024

1 DeWayne Campbell
Technical Project Officer - YMP
US Bureau of Reclamation
Code D-3700
P.O. Box 25007
Denver, CO 80225

1 J. M. LaMonaca
Records Specialist
US Geological Survey
421 Federal Center
P.O. Box 25046
Denver, CO 80225

1 W. R. Keefer - USGS
913 Federal Center
P.O. Box 25046
Denver, CO 80225

1 M. D. Voegele
Technical Project Officer - YMP
SAIC
101 Convention Center Drive
Suite 407
Las Vegas, NV 89109

1 Paul Eslinger, Manager
PASS Program
Pacific Northwest Laboratories
P.O. Box 999
Richland, WA 99352

1 A. T. Tamura
Science and Technology Division
OSTI
US Department of Energy
P.O. Box 62
Oak Ridge, TN 37831

1 Carlos G. Bell, Jr.
Professor of Civil Engineering
Civil and Mechanical Engineering Dept.
University of Nevada, Las Vegas
4505 S. Maryland Parkway
Las Vegas, NV 89154

1 P. J. Weeden, Acting Director
Nuclear Radiation Assessment Div.
US EPA
Environmental Monitoring Sys. Lab
P.O. Box 93478
Las Vegas, NV 89193-3478

1 ONWI Library
Battelle Columbus Laboratory
Office of Nuclear Waste Isolation
505 King Avenue
Columbus, OH 43201

1 D. Hedges, Vice President, QA
Roy F. Weston, Inc.
4425 Spring Mountain Road
Suite 300
Las Vegas, NV 89102

1 D. L. Fraser, General Manager
Reynolds Electrical & Engineering
Company, Inc.
MS 555
P.O. Box 98521
Las Vegas, NV 89193-8521

1 B. W. Colston, President & Gen. Mgr.
Las Vegas Branch
Raytheon Services Nevada
MS 416
P.O. Box 95487
Las Vegas, NV 89193-5487

1 R. L. Bullock
Technical Project Officer - YMP
Raytheon Services Nevada
Suite P-250, MS 403
101 Convention Center Drive
Las Vegas, NV 89109

1 C. H. Johnson
Technical Program Manager
Agency for Nuclear Projects
State of Nevada
Evergreen Center, Suite 252
1802 N. Carson Street
Carson City, NV 89710

1 John Fordham
Water Resources Center
Desert Research Institute
P.O. Box 60220
Reno, NV 89506

1 David Rhode
Desert Research Institute
P.O. Box 60220
Reno, NV 89506

1 Eric Anderson
Mountain West Research Southwest Inc.
2901 N. Central Avenue, #1000
Phoenix, AZ 85012-2730

1 The Honorable Cyril Schank
Chairman
Churchill County Board of
Commissioners
190 W. First Street
Fallon, NV 89406

1 T. Hay, Executive Assistant
Office of the Governor
State of Nevada
Capitol Complex
Carson City, NV 89710

3 R. R. Loux
Executive Director
Agency for Nuclear Projects
State of Nevada
Evergreen Center, Suite 252
1802 N. Carson Street
Carson City, NV 89710

1 Brad Mettam
Inyo County Yucca Mountain
Repository Assessment Office
Drawer L
Independence, CA 93526

1 Lander County Board of
Commissioners
315 South Humbolt
Battelle Mountain, NV 89820

1 Vernon E. Poe
Office of Nuclear Projects
Mineral County
P.O. Box 1026
Hawthorne, NV 89415

1 Les W. Bradshaw
Program Manager
Nye County Repository
P.O. Box 429
Tonopah, NV 89049

1 Florindo Mariani
White Pine County Nuclear
Waste Project Office
457 Fifth Street
Ely, NV 89301

1 Judy Foremaster
City of Caliente Nuclear Waste
Project Office
P.O. Box 158
Caliente, NV 89008

1 Philip A. Niedzielski-Eichner
Nye County Nuclear Waste
Repository Project Office
P.O. Box 221274
Chantilly, VA 22022-1274

1 Dennis Bechtel, Coordinator
Nuclear Waste Division
Clark County Department of
Comprehensive Planning
301 E. Clark Avenue, Suite 570
Las Vegas, NV 89101

1 Juanita D. Hoffman
Nuclear Waste Repository
Oversight Program
Esmeralda County
P.O. Box 490
Goldfield, NV 89013

1 Eureka County Board of Commissioners
Yucca Mountain Information Office
P.O. Box 714
Eureka, NV 89316

1 Economic Development Dept.
City of Las Vegas
400 E. Stewart Avenue
Las Vegas, NV 89101

1 Community Planning & Development
City of North Las Vegas
P.O. Box 4086
North Las Vegas, NV 89030

1 Community Development & Planning
City of Boulder City
P.O. Box 61350
Boulder City, NV 89006

1 Commission of European Communities
200 Rue de la Loi
B-1049 Brussells
BELGIUM

2 M. J. Dorsey, Librarian
YMP Research & Study Center
Reynolds Electrical & Engineering
Company, Inc.
MS 407
P.O. Box 98521
Las Vegas, NV 89193-8521

1 Amy Anderson
Argonne National Laboratory
Building 362
9700 S. Cass Avenue
Argonne, IL 60439

1 Steve Bradhurst
P.O. Box 1510
Reno, NV 89505

1 Michael L. Baughman
35 Clark Road
Fiskdale, MA 01518

1 Glenn Van Roekel
Director of Community Development
City of Caliente
P.O. Box 158
Caliente, NV 89008

1 Jason Pitts
Lincoln County Nuclear Waste
Project Office
Lincoln County Courthouse
Pioche, NV 89043

1 Ray Williams, Jr.
P.O. Box 10
Austin, NV 89310

1 Nye County District Attorney
P.O. Box 593
Tonopah, NV 89049

1 William Offutt
Nye County Manager
Tonopah, NV 89049

1 Charles Thistlethwaite, AICP
Associate Planner
Inyo County Planning Department
Drawer L
Independence, CA 93526

1 R. F. Pritchett
Technical Project Officer - YMP
Reynolds Electrical & Engineering
Company, Inc.
MS 408
P.O. Box 98521
Las Vegas, NV 89193-8521

1 Dr. Moses Karakouzian
1751 E. Reno, #125
Las Vegas, NV 89119

1 Lawrence Berkeley Laboratory
Attn: K. Pruess
Earth Sciences Division
Berkeley, CA 94720

1 Los Alamos National Laboratory
Attn: G. Zyvoloski
P.O. Box 1663
Los Alamos, NM 87545

1 R. W. Nelson
INTERA
101 Convention Center Drive
Suite 540
Las Vegas, NV 89109

1 L. D. Stewart
Praxis Engineering Services, Inc.
160 Portola Dr.
Suite 205
San Francisco, CA 94131

1 M. Reeves
INTERA
6850 Austin Center Blvd.
Suite 30
Austin, TX 78731

1 University of California, Berkeley
Attn: K. S. Udell
Department of Mechanical Engineering
Berkeley, CA 94720

1 University of Washington
Attn: D. F. McTigue
Dept. of Geological Sciences, AJ-20
Seattle, WA 98195

	MS	
1	0841	P. J. Hommert, 1500
1	0841	J. H. Biffle, 1503
1	0828	E. D. Gorham, 1504 (Route to 1553/1554)
1	0827	R. T. McGrath, 1511
1	0827	C. E. Hickox, 1511
1	0827	P. L. Hopkins, 1511
10	0827	M. J. Martinez, 1511
1	0834	A. C. Ratzel, 1512
1	0835	R. D. Skocypec, 1513
1	0826	W. Hermina, 1514
1	0826	C. C. Wong, 1515
1	1324	P. B. Davies, 6115
1	1324	R. J. Glass, 6115
1	1324	C. K. Ho, 6115
1	1324	S. W. Webb, 6115
1	1320	M. D. Siegel, 6119
1	1327	F. Bingham (Acting), 6300
1	1326	H. A. Dockery, 6312
1	1326	G. E. Barr, 6312
1	1326	J. H. Gauthier, 6312
1	1326	M. L. Wilson, 6312
1	1325	E. E. Ryder, 6313
1	1345	D. Updegraff, 6331
1	1328	M. E. Fewell, 6342
1	1328	M. G. Marietta, 6342
1	0719	J. M. Phelan, 6621
1	9043	R. H. Nilson, 8745

2	1330	C. B. Michaels, 6352 100/1.2.5.4.1/SAND94-0379/QA
20	1330	WMT Library, 6352
1	9018	Central Technical Files, 8523-2
5	0899	Technical Library, 13414
1	0619	Print Media, 12615
2	0100	Document Processing, 7613-2 for DOE/OSTI